


Biophysical parameters and extreme air temperature indices in the Cerrado-Amazonia transition

Marlus Sabino¹ 

Jonh Billy da Silva¹ 

Rayanna de Oliveira Costa¹ 

Leilane Gomes Duarte¹ 

Adilson Pacheco de Souza^{1, 2} 

Keywords:

Albedo
Radiation
Heat flux
Climate changes
Soil use

Abstract

This paper aimed to evaluate the changes in biophysical parameters and trends in annual extremes of air temperature in Sinop, Mato Grosso, Brazil, using data from automatic weather stations (AWS) installed in rural and urban areas of the municipality. Changes in land use, surface albedo, radiation balance (R_n), sensible heat (H), and latent heat (LE) were estimated from Landsat 5 and Landsat 8 satellite images obtained in 2007, 2011 and 2017. With RCLIMDEX software, the trends in six extreme indices of annual maximum and minimum temperatures were calculated with least-squares calibration and statistical significance assessed by Fisher test at a significance level (α) equal to 0.05. Through the years changes in land use and biophysical parameters like increase of albedo and reduction of R_n were observed in the rural area, while at the urban station (UFMT Sinop) the inversion of LE and H partition was observed. The extreme indices indicated an increasing tendency towards extreme temperatures in the urban area, with significant changes occurring in the indices T_{Nx} , DTR , T_{n90p} , and T_{x90p} . In the last decade, with the expansion of the urban area of Sinop, Mato Grosso - Brazil, fluctuations in trends of temperature extreme indices were observed, and are attributed to changes in land use and biophysical parameters.

¹Graduate Program in Environmental Physics, Physic Institute, Federal University of Mato Grosso, Cuiabá, Mato Grosso, Brasil. marlussabino@gmail.com; jonhbilly9@gmail.com; rayanna.oli.costa@gmail.com; leilane@fisica.ufmt.br

²Institute of Agricultural and Environmental Sciences, Federal University of Mato Grosso (UFMT), Sinop, Mato Grosso, Brasil. pachecoufmt@gmail.com

INTRODUCTION

In recent years, evidence of anthropogenic global warming has gained strength with the development of numerical models to predict the increase in air temperature due to greenhouse gas emissions. However, the long-term forecast is still uncertain, with divergences on the precise effects of environmental changes on climate (JUNGES; MASSONI, 2018).

Tropical forests ecosystems, due to physical and biological interactions in the soil-plant-atmosphere system, such as control of the carbon cycle and water availability to the atmosphere by evapotranspiration processes, play a key role in climate regulation at the local and regional scale (ARTAXO et al., 2014; DOUGHTY et al., 2015). However, this dynamic balance, in the regions of the Amazon-Cerrado (Rainforest-Savanna) biome transition, is subject to the effects of human actions such as the growth of urban centers and land management associated with deforestation, fire disturbance, and expansion of agriculture and pasture areas (NOBRE et al., 2007; ARAÚJO et al., 2015).

Replacement of natural forests by monocultures and urban centers can cause changes in the local and regional climate as a result of shifts in the surface albedo and energy exchanges between surface and atmosphere (MARTINS et al., 2015), which can impact air and soil temperature, as well as evapotranspiration.

Since air temperature is easier to obtain than other meteorological parameters, it has frequently been used to identify climate changes by associating its fluctuations with shifts in the trends of extreme event indices related to global warming (MARENGO et al., 2007). In Brazil, several studies have used the extreme temperature indices proposed by the World Meteorological Organization (WMO) to assess local climate change (DANTAS et al., 2015; SANTOS et al., 2012; SANTOS et al., 2020; SILVA et al., 2015; SILVA et al., 2017). However, most studies have concentrated on the South and Southeast of the country, where there is a greater number of weather stations with quality-controlled and long-range meteorological datasets.

The city of Sinop, Mato Grosso - Brazil, a result of the occupation policy of the Brazilian

Legal Amazon developed by the federal government in the 1970s, has 142,996 inhabitants (IBGE, 2020). It is located in the northern region of Mato Grosso, with an area of 3,194.4 km² and an urban perimeter of 17 km². The city is located in the Teles Pires River basin (between the Upper and Middle Teles Pires regions) and its economy is dominated by agriculture and forestry. Sinop is a planned city incorporating modern urban criteria like a grid plan street design and a large average green space of 27.00 m² per inhabitant. However, in recent years the city has experienced a boom in its urban and agricultural area that has led to changes in land occupation and, consequently, in regional biophysical variables.

This study aimed to assess changes in biophysical parameters (albedo, radiation balance, latent heat flow, and sensitive heat flow), land use and occupation, and their implications for extreme air temperature trends in the urban and rural areas of the municipality of Sinop, located in the Cerrado-Amazon transition region, Northern Mato Grosso.

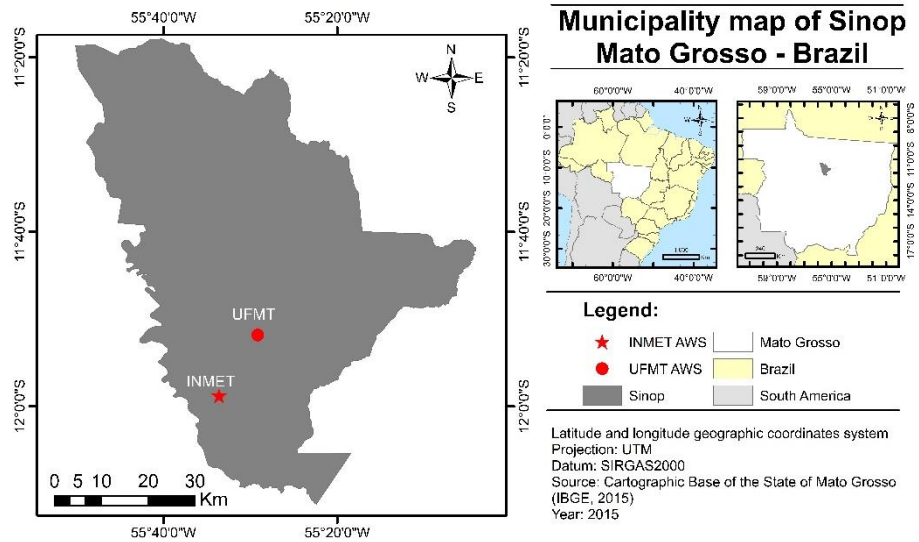
MATERIAL E METHODS

Study location

The daily series of maximum and minimum temperature data were obtained from the automatic weather station code A917 belonging to the Instituto Nacional de Meteorologia (INMET, in Portuguese), the federal institute responsible for the main meteorology net in Brazil, installed at latitude -11° 58', longitude -55° 34' and altitude 367 m (INMET, 2018), and that of the Universidade Federal de Mato Grosso (UFMT - Campus Universitário de Sinop), installed at latitude -11° 51', longitude -55° 29' and altitude 371 m (Figure 1). The stations are located, respectively, in rural and urban areas of the municipality of Sinop, with databases containing the years of 2007 to 2017 (INMET) and 2011 to 2016 (UFMT).

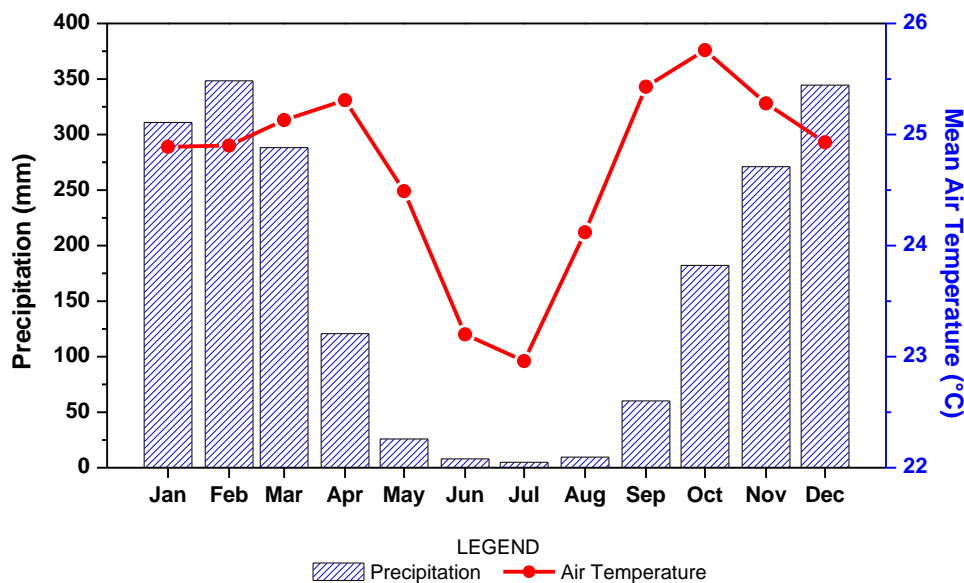
According to the Koppen classification, the climatic type in the region is Aw - humid tropical climate, with a well-defined dry season (May to September), average annual precipitation around 1,970 mm and average annual temperature of 24.70 °C (SOUZA et al., 2013) (Figure 2).

Figure 1. Location of INMET and UFMT automatic weather stations, Sinop - MT, Brazil



Org.: From the authors, 2019.

Figure 2. Climogram of the Gleba Celeste weather station located in the middle north region of Mato Grosso state (climatological normal: 1972 at 2010).



Org.: Adapted from Souza et al. (2013).

Image acquisition and processing

The evaluation of changes in land use and occupation, as well as changes in albedo (α), radiation balance (R_n), latent heat flow (LE), and sensitive heat flow (H), was carried out with the help of remote sensing tools, using six images of surface reflectance and brightness temperature from the Operational Land Imager (OLI), Thermal Infrared Sensor (TIRS) and Thematic Mapper (TM), generated onboard the Landsat 5 and Landsat 8 satellites at the orbit 226 point 68, and

the orbit 227 point 68, obtained from the US Geological Survey (USGS, 2018). Since the presence of clouds can cause errors in the estimates of energy balance, images from August (dry season) in the years 2007, 2011, and 2017 were used.

The surface reflectance images have undergone radiometric correction, atmospheric correction, systematic geometric correction, and precision correction using ground control chips, as well as a digital elevation model to correct parallax error due to the local topographic relief

(CLAVERIE et al., 2015).

Estimates of biophysical parameters

The albedo, radiation balance, sensitive heat flow, and latent heat flow were obtained as part of the R-SSEB Algorithm (Simplified Modeling for Energy Balance Estimation to the Regional Scale Surface) proposed by Araújo et al. (2017). The surface albedo was calculated according to Equation 1, proposed by Tasumi et al. (2008).

$$\alpha_{sup} = \frac{\alpha_{toa} - \alpha_{atm}}{\tau_{sw}^2} \quad (1)$$

where: α_{atm} is the portion of solar radiation reflected by the atmosphere, 0.03 was adopted according to Bastiaanssen (2000); τ_{sw}^2 is the atmospheric transmittance; and α_{toa} represents the albedo of the surface, without atmospheric correction.

The surface albedo, without atmospheric correction, was obtained through a linear combination of the spectral reflectances of the bands (ρ) 2, 3, 4, 5, 6, and 7, Equation 2. Atmospheric transmittance for clear skies, Equation 3, was determined as proposed by Allen et al. (2007).

$$\alpha_{toa} = 0.300\rho_2 + 0.277\rho_3 + 0.233\rho_4 + 0.143\rho_5 + 0.036\rho_6 + 0.012\rho_7 \quad (2)$$

$$\tau_{sw} = 0.35 + 0.627 \exp \left[\frac{-0.00146P}{K_t \cos\theta_{hor}} - 0.075 \left(\frac{W}{\cos\theta_{hor}} \right)^{0.4} \right] \quad (3)$$

where: P is the atmospheric pressure kPa; W is precipitable water in the atmosphere; $\cos\theta_{hor}$ is the solar zenith angle on a horizontal surface; Kt is the turbidity coefficient (Kt = 1.0 for clean air and Kt = 0.5 for extremely cloudy, dusty or polluted air).

The NDVI (Normalized Difference Vegetation Index) that serves as a measure of vegetation condition assessment is given by Equation 4, as proposed by Huete et al. (2002).

$$NDVI = \frac{\rho_{IVP} - \rho_{VER}}{\rho_{IVP} + \rho_{VER}} \quad (4)$$

where: ρ_{IVP} is the reflectance of the near infrared; and ρ_{VER} is the reflectance of the red.

The daily radiation balance (Rn24), which represents the sum of radiative fluxes to the

surface in 24 hours, was obtained by calculating the upward and downward fluxes of longwave and shortwave radiation acting on the soil-plant-atmosphere system, Equation 5.

$$Rn = R_{s\downarrow}(1 - \alpha_{sup}) - R_{L\uparrow} + R_{L\downarrow} - (1 - \varepsilon_0)R_{L\downarrow} \quad (5)$$

where: $R_{s\downarrow}$ is the incident short-wave radiation (Wm^{-2}), α_{sup} is the surface albedo (dimensionless), $R_{L\downarrow}$ is the long-wave radiation emitted by the atmosphere towards the surface (Wm^{-2}), $R_{L\uparrow}$ is the radiation of long waves emitted by the surface; and ε_0 is the emissivity.

Since incident shortwave solar radiation ($R_{s\downarrow}$) is the main source of energy for evapotranspiration (ET), Equation 5 can be simplified according to Equation 6, in which global radiation represents the sum of short radiation (direct and diffuse) reaching the Earth's surface ($W m^{-2}$), being attenuated, along with the longwave components, by the properties of atmospheric transmissivity and surface albedo.

$$Rn_{24} = Rg_{24} \times (1 - \alpha_{sup}) - (110 \times \tau_{24}) \quad (6)$$

where: Rg_{24} is the global daily radiation ($W m^{-2}$) obtained from an automatic meteorological station in the INMET network near the study area; α_{sup} is the surface albedo; and τ_{24} is the average daily transmissivity of the atmosphere.

The components of the energy balance are obtained from the Rn estimate described above. Initially, the heat flow in the soil (G) was calculated through parameterizations. Then, the sensible heat (H) and latent heat (LE) fluxes were determined by the evaporative fraction (EF).

The G value was computed according to Eq. (7) developed by Bastiaanssen (2000):

$$G = \left[\frac{T_s}{\alpha} (0.0038\alpha + 0.0074\alpha^2)(1 - 0.98 NDVI^4) \right] R_n \quad (7)$$

where: T_s is the surface temperature ($^{\circ}C$); α is the surface albedo (dimensionless); NDVI is the vegetation index (dimensionless); R_n is the radiation balance (Wm^{-2}).

In the R-SSEB model, the evaporative fraction (EF) is calculated using the average of at least three hot pixels and three cold pixels identified in the NDVI and T_s maps (SENAY et al., 2007). Assuming that the hot pixels have small ET values and the cold pixels represent the maximum

ET over the entire study area, the average of each set of pixels can be used to calculate the EF for all the pixels in the scene from Equation 8 developed by Senay et al. (2013):

$$FE = \frac{T_H - T_S}{T_H - T_C} \quad (8)$$

where: T_H is the average of the hot pixels, T_C is the average of the cold pixels and T_S is the surface temperature.

Once the FE was determined, the sensible (H) and latent (LE) heat fluxes were calculated according to Eqs. (9) and (10) (ROERINK et al., 2000; SOBRINO et al., 2007):

$$H = (1 - FE)(Rn - G) \quad (9)$$

$$LE = FE(Rn - G) \quad (10)$$

The means and 95% confidence intervals of the biophysical parameters (α , Rn, H, LE) were calculated by bootstrapping with 1000 iterations

the randomized resamplings with substitution (EFRON; TIBSHIRANI, 1993) and compared using the Kruskal-Wallis test, $\alpha = 0.05$.

Extreme air temperature indices

Eleven extreme air temperature indices (Table 1) were calculated using the Rclimindex software, developed for the R language by the National Climate Data Center (NCDC) of the National Oceanic and Atmospheric Administration (NOAA) as documented by Easterling et al. (2003); Tank et al. (2009), for being recommended in the analysis of extreme climatic indices that assist in monitoring and detecting climate changes.

A prerequisite for the calculation of the indices is the quality control of the data (ZHANG; YANG, 2004), which proceeds in 3 stages: a) replacement of missing data; b) replacement of non-representative values ($T_{max} < T_{min}$); and c) identification of extreme values (outliers) based on a predetermined number of standard deviations.

Table 1. Extreme air temperature indexes evaluated in the Sinop region, MT.

Indice	Definition	Unidade
Tn10p	Annual percentage of days on which TN < percentil 10	%
Tx10p	Annual percentage of days on which TX < percentil 10	%
Tn90p	Annual percentage of days on which TN > percentil 90	%
Tx90p	Annual percentage of days on which TX > percentil 90	%
CSDI	Maximum number of consecutive days in the year with TN <	Days
WSDI	Maximum number of consecutive days in the year with TX >	Days
TXx	Maximum annual value of the maximum daily temperature	°C
TXn	Annual minimum value of maximum temperature	°C
TNx	Maximum annual value of the minimum daily temperature	°C
TNn	Minimum annual value of the minimum daily temperature	°C
DTR	Mean annual difference between TX e TN	°C

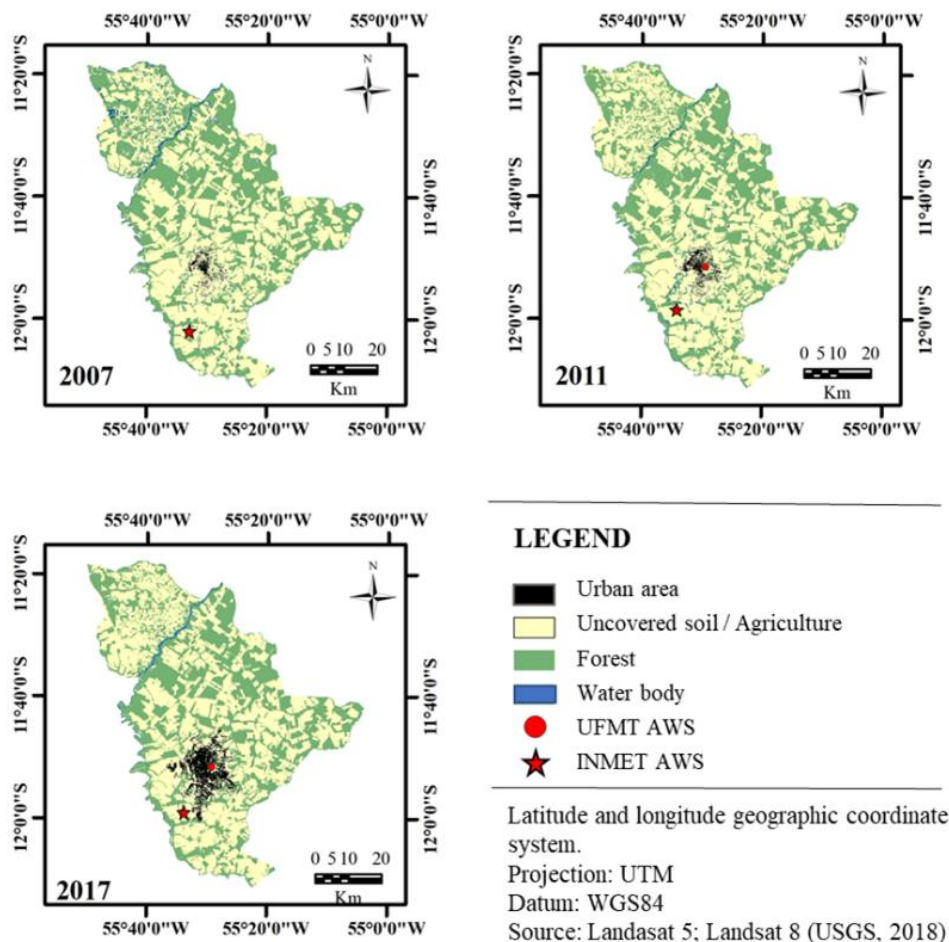
Org.: From the authors, 2019.

After the quality control test, the data undergo homogeneity analysis to detect possible discontinuities or displacements in the time series data records. The homogeneity test is based on the maximum penalized t-test (WANG et al., 2007) and maximum penalized F test (WANG, 2008), which are embedded in a recursive test algorithm. The annual trends in the climatic extreme indices were obtained by regression analysis using the least-squares method and statistical significance was determined by the Fisher's test.

RESULTS AND DISCUSSION

The analysis of the change in land use showed a gradual reduction in native forest areas, which went from 41.76% to 39.47% of the total area of the municipality, as well as an increase in agricultural areas, whose percentage went from 55.51% to 56.22%. However, the main change occurred due to the growth of the urban center, which increased by 408% in a decade, with the most accentuated growth having occurred between 2011 and 2017 (Table 2; Figure 3).

Figure 3. Map of land use of the municipality of Sinop - MT for the years 2007, 2011 and 2017.



Org.: From the authors, 2019.

Table 2. Percentage of area of different land use, between 2007, 2011, and 2017, in the municipality of Sinop - MT.

Land use	Year		
	2007	2011	2017
Urban area	0.71	1.05	3.61
Uncovered soil / Agriculture	55.51	57.74	56.22
Forest	41.76	39.96	39.47

Org.: From the authors, 2019.

Similar to land use, biophysical parameters also changed, mainly in the urban area. The albedo near the UFMT station increased from 0.25 to 0.45 between 2007 and 2017, being 31% higher than the estimate at INMET station in 2017 (rural area). Inversely to albedo, the net radiation, in the period, decreased by 30.78% and 14.29% for the UFMT and INMET stations, respectively (Table 3).

At the INMET station, the portions of the energy flow remained similar throughout the study period, corresponding to latent heat flow of 52.60% (2007) and 53.91% (2017) of the radiation

balance, and to sensitive heat flow of 35.04% (2007) and 34.40% (2017). The urbanization process, however, was responsible for changes in the parcel of energy destined for each flow. For the UFMT station an increase in the partition of sensitive heat flow, which went from 28.75% (2007) to 53.94% (2017), and reduced latent heat flow, whose percentage decreased from 58.99% (2007) to 25.23% (2017) (Table 3).

The results of the air temperature extreme indices at the meteorological stations are presented in Figure 4. At the INMET station, no significant trends were found (p-value <0.10) in

the indices related to changes in the maximum and minimum temperature values (TXx, TXn, TNx, TNn, and DTR). However, at the UFMT station, there were significant increasing trends of 0.34 °C in the maximum air temperature (TNx) and 0.32 °C in the daily temperature amplitude (DTR).

Regarding the changes in days with extreme

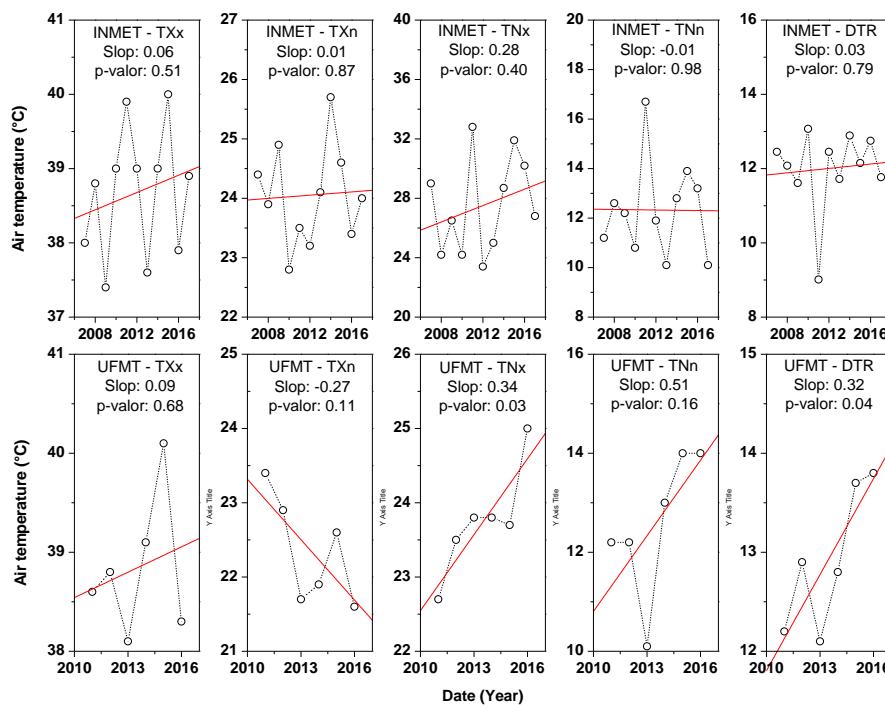
temperatures, an increasing trend in days with higher maximum and minimum temperatures was observed at the INMET station, given by the indices Tx90p (0.91%) and Tn90p (1.15%). Such changes were even more pronounced at the UFMT station, where increases of 4.84% (Tn90p) and 3.15% (Tx90p) were observed (Figure 5).

Table 3. biophysical parameters changes, between 2007 and 2017, at the two AWS in the municipality of Sinop - MT.

biophysical parameters	UFMT			INMET		
	2007	2011	2017	2007	2011	2017
α	0.25 (0.1)	0.43 (0.1)	0.45 (0.1)	0.20 (0.1)	0.24 (0.1)	0.31 (0.1)
Rn	1862.3 (17.2)	1330.8 (17.2)	1289.0 (17.2)	1875.5 (16.9)	1621.2 (16.9)	1607.4 (16.9)
LE	1098.6 (23.2)	419.1 (23.2)	325.2 (23.2)	986.5 (22.8)	767.2 (22.8)	866.5 (22.8)
H	535.5 (12.1)	648.2 (12.1)	695.3 (12.1)	657.2 (11.9)	618.7 (11.9)	553.0 (11.9)

Values in parentheses represent the difference between the confidence interval and the mean. Org.: From the authors, 2019.

Figure 4. Extreme indices of maximum and minimum air temperatures at INMET and UFMT weather stations.



Org.: From the authors, 2019.

Increasing trends in indices related to temperature were also found by Marengo and Camargo (2008) at 27 stations in southern Brazil, between 1960 and 2002, with increases of 0.5 to 0.8 °C over a decade for minimum temperatures and of 0.4 °C over a decade for

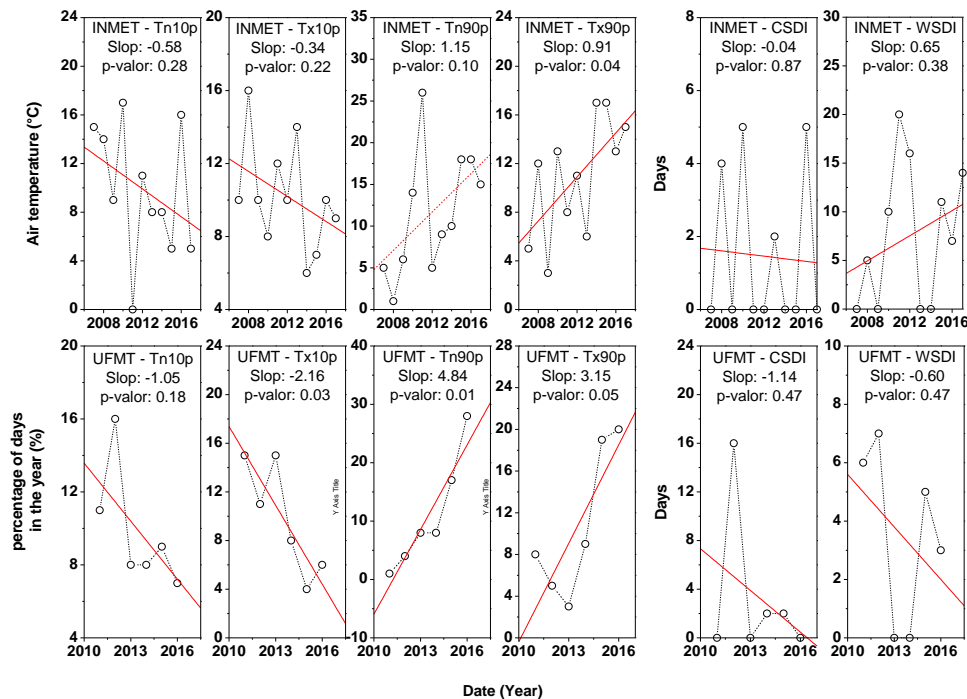
maximum temperatures. Similarly, the IPCC synthetic report (2007), which presented an overview of average annual temperatures on the South American continent, showed a 0.5 °C heating trend for the period from 1950 to 2000.

The increase in air temperature observed

mainly at the UFMT station is related, among other factors, to changes in land occupation. Among these changes in land use, deforestation is a major factor affecting the climate, according to Foley et al. (2005). The conversion of native vegetation to areas of agricultural activities and

urban centers is responsible for variations in the temperature, since it causes a reduction in evapotranspiration processes (HUNKE et al., 2015), changing the portions and the magnitude of the radiation balance, albedo, and latent and sensitive heat fluxes (RODRIGUES et al., 2013).

Figure 5. Indices related to the number of days with extreme values of maximum and minimum air temperatures in the meteorological stations of INMET and UFMT.



Org.: From the authors, 2019.

The absence of vegetation cover causes a greater reflection of shortwave radiation and greater emission of longwave radiation, reducing the surface radiation balance (ANDRADE et al., 2014) and making energy available to the environment to be used primarily in the flow of sensitive heat, thereby heating the soil and air (BIUDES et al., 2015). In contrast, in environments with vegetation, since most of the radiation balance is used in evapotranspiration processes (latent heat), there is a trend towards increased water vapor content and reduced maximum temperature.

These results, however, should be seen as preliminary since it is not possible to attribute the differences among temperature trends exclusively to land use and the expansion of urban areas, in addition to the fact that the database does not correspond to the 30 years of measurements recommended by OMM for climatic characterization (SILVA et al., 2017).

FINAL CONSIDERATIONS

Changes in land use and occupation between the years 2007 and 2017 were responsible for an increase of 80% and 55% in the surface albedo and a reduction of 30.78% and 14.29% in the radiation balance at the urban (UFMT) and rural (INMET) weather stations in the municipality of Sinop-MT, respectively.

The energy portion destined for H and LE remained constant at the rural station (INMET). In the urban area (UFMT) there was an inversion of the energy portions of the radiation balance with an increase in H (air heating) and a reduction in LE (evapotranspiration).

The station in the urban area (UFMT) showed a higher increase in the temperature extreme indices TNx ($0.34\text{ }^{\circ}\text{C year}^{-1}$), DTR ($0.32\text{ }^{\circ}\text{C year}^{-1}$), Tn90p (4.84%) and Tx90p (3.15%), indicating that the urbanization of the municipality is beginning to change the local environmental biophysical parameters.

In future analyses, it is recommended that meteorological stations in other parts of the municipality be incorporated, since urban expansion is taking place in varying directions.

ACKNOWLEDGMENT

To the National Meteorological Institute (INMET) for making the databases available. This work was carried out with the support of the Coordination for the Improvement of Higher Education Personnel - Brazil (CAPES) - Financing Code 001.

REFERENCES

- ALLEN, R. G.; TASUMI, M.; TREZZA, R. Satellite-based energy balance for mapping evapotranspiration with internalized calibration (METRIC) - Model. **Journal of Irrigation and Drainage Engineering**, v. 133, p. 380-394, 2007. DOI: [10.1061/\(ASCE\)0733-9437\(2007\)133:4\(380\)](https://doi.org/10.1061/(ASCE)0733-9437(2007)133:4(380))
- ANDRADE, A. M. D.; MOURA, M. A. L.; SANTOS, A. B.; CARNEIRO, R. G.; JUNIOR, R. S. Radiação fotossinteticamente ativa incidente e refletida acima e abaixo do dossel de Floresta de Mata Atlântica em Coruripe, Alagoas. **Revista Brasileira de Meteorologia**, v. 29, n. 1, p. 68-79, 2014. <https://doi.org/10.1590/S0102-77862014000100007>
- ARAÚJO, F. C. D.; SANTOS, C. A. C.; NASCIMENTO, F. C. A. Estudo dos índices extremos de temperatura na bacia hidrográfica do baixo rio Colorado-EUA. **Revista Brasileira de Meteorologia**, v. 30, n. 1, 2015. <https://doi.org/10.1590/0102-778620120530>
- ARAÚJO, A. L.; SILVA M. T.; SILVA, B. B.; SANTOS, C. A. C.; AMORIM, M. R. B. Modelagem Simplificada Para Estimativa do Balanço de Energia à Superfície em Escala Regional (R-SSEB). **Revista Brasileira de Meteorologia**, v. 32, n. 3, p. 433-446, 2017. <https://doi.org/10.1590/0102-77863230010>
- ARTAXO, P.; DIAS, M. A. F. D. S.; NAGY, L.; LUIZÃO, F. J.; CUNHA, H. B. D.; QUESADA, C. A.; MARENGO, J. A.; KRUSCHE, A. Perspectivas de pesquisas na relação entre clima e o funcionamento da Floresta Amazônica. **Ciência e Cultura**, v. 66, n. 3, p. 41-46, 2014. <http://dx.doi.org/10.21800/S0009-67252014000300014>
- BASTIAANSEN, W. G. M. SEBAL-based sensible and latent heat fluxes in the irrigated Gediz Basin, Turkey. **Journal of Hydrology**, v. 229, p. 87-100, 2000. [https://doi.org/10.1016/S0022-1694\(99\)00202-4](https://doi.org/10.1016/S0022-1694(99)00202-4)
- BIUDES, M. S.; VOURLITIS, G. L.; MACHADO, N. G.; DE ARRUDA, P. H. Z.; NEVES, G. A. R.; DE ALMEIDA LOBO, F.; NEALE, C. M. U.; NOGUEIRA, J. S. Patterns of energy exchange for tropical ecosystems across a climate gradient in Mato Grosso, Brazil. **Agricultural and Forest Meteorology**, v. 202, p. 112-124, 2015. <https://doi.org/10.1016/j.agrformet.2014.12.008>
- CLAVERIE, M.; VERMOTE, E. F.; FRANCH, B.; MASEK, J. G. Evaluation of the Landsat-5 TM and Landsat-7 ETM + surface reflectance products. **Remote Sensing of Environment**, v. 169, p. 390-403, 2015. <https://doi.org/10.1016/j.rse.2015.08.030>
- DANTAS, L. G.; SANTOS, C. A. C. D.; OLINDA, R. A. D. Tendências anuais e sazonais nos extremos de temperatura do ar e precipitação em Campina Grande-PB. **Revista Brasileira de Meteorologia**, v. 30, n. 4, p. 423-434, 2015. <https://doi.org/10.1590/0102-778620130088>
- DOUGHTY, C. E.; METCALFE, D. B.; GIRARDIN, C. A.; AMEZQUITA, F. F.; DURAND, L.; HUASCO, W. H.; ESPEJO, J. E. S.; MURAKAMI, A. A.; COSTA, M. C.; COSTA, A. C. L.; ROCHA, W.; MEIR, P.; GALBRAITH, D.; MALHI, Y. Source and sink carbon dynamics and carbon allocation in the Amazon basin. **Global Biogeochemical Cycles**, v. 29, n. 5, p. 645-655, 2015. <https://doi.org/10.1002/2014GB005028>
- EASTERLING, D. R.; ALEXANDER, L. V.; MOKSSIT, A.; DETEMMERMAN, V. CCI/CLIVAR workshop to develop priority climate indices. **Bulletin of the American Meteorological Society**, v. 84, n. 10, p. 1403-1407, 2003. DOI: [10.1175/BAMS-84-10-1403](https://doi.org/10.1175/BAMS-84-10-1403)
- EFRON, B.; TIBSHIRANI, R. J. **An introduction to the bootstrap**. New York: Chapman & Hall; 1993. 443 p.
- FOLEY, J. A.; FRIES, R.; ASNER, G. P.; BARFORD, C.; BONAN, G.; CARPENTER, S. R.; CHAPIN, F. S.; COE, M. T.; DAILY, G. C.; GIBBS, H. K.; HELKOWSKI, J. H.; HOLLOWAY, T.; HOWARD, E. A.; KUCHARIK, C. J.; MONFREDA, C.; PATZ, J. A.; PRENTICE, C. RAMANKUTTY, N.; SNYDER, P. K. Global consequences of land use. **Science**, v. 309, n. 5734, p. 570-574, 2005. DOI: [10.1126/science.1111772](https://doi.org/10.1126/science.1111772)
- HUETE, A.; DIDAN, K.; MIURA, T.; RODRIGUEZ, E.P.; GAO, X.; FERREIRA, L. G. Overview of the radiometric and biophysical

- performance of the MODIS vegetation indices. **Remote Sensing of Environment**, v. 83, p. 195-213, 2002. [https://doi.org/10.1016/S0034-4257\(02\)00096-2](https://doi.org/10.1016/S0034-4257(02)00096-2)
- HUNKE, P.; ROLLER, R.; ZEILHOFER, P.; SCHRÖDER, B.; MUELLER, E.N. Soil changes under different land-uses in the Cerrado of Mato Grosso, Brazil. **Geoderma Regional**, v. 4, p. 31-43, 2015. <https://doi.org/10.1016/j.geodrs.2014.12.001>
- IBGE - Instituto Brasileiro de Geografia e Estatística. **Cidades e Estados: Sinop (código 5107909)**. Disponível em: <<https://www.ibge.gov.br/cidades-e-estados/mt/sinop.html>>. Acesso em: 30 de julho de 2020.
- INMET - Instituto Nacional de Meteorologia. **Estação Meteorológica de Observação de Superfície Automática**. 2018 Disponível em: <<http://www.inmet.gov.br>>. Acesso em: 06 de julho de 2018.
- INTERGOVERNMENTAL PANEL ON CLIMATE CHANGE - IPCC. **Climate Change 2007: Synthesis Report**. IPCC Plenary XXVII, Valencia, Spain, 2007. 73 p.
- JUNGES, A. L.; MASSONI, N. T. O Consenso Científico sobre Aquecimento Global Antropogênico: Considerações Históricas e Epistemológicas e Reflexões para o Ensino dessa Temática. **Revista Brasileira de Pesquisa em Educação em Ciências**, v. 18, n. 2, p. 455-491, 2018. <https://doi.org/10.28976/1984-2686rbpec2018182455>
- MARTINS, A. L.; CUNHA, C. R.; RODRIGUES, P. V. M.; MORAIS, D. V. H.; GOMES, M. N.; ALMEIDA, L. F.; BIUDES, M. S. Mudanças em índices biofísicos devido à alteração da cobertura do solo em área nativa de Cerrado em Mato Grosso. **Ciência e Natura**, v. 37, n. 3, 2015. <http://dx.doi.org/10.5902/2179460X16145>
- MARENGO, J. A.; ALVES, L.; VALVERDE, M.; ROCHA, R.; LABORBE, R. **Eventos extremos em cenários regionalizados de clima no Brasil e América do Sul para o Século XXI**: Projeções de clima futuro usando três modelos regionais. Relatório 5. São Paulo: Ministério do Meio Ambiente, 2007. 77 p.
- MARENGO, J. A.; CAMARGO, C. C. Surface air temperature trends in Southern Brazil for 1960–2002. **International Journal of Climatology: Journal of the Royal Meteorological Society**, v. 28, p. 893-904, 2008. <https://doi.org/10.1002/joc.1584>
- NOBRE, C. A.; SAMPAIO, G.; SALAZAR, L. Mudanças climáticas e Amazônia. **Ciência e Cultura**, v. 59, n. 3, p. 22-27, 2007.
- RODRIGUES, T. R.; PAULO, S. R.; NOVAIS, J. W.; CURADO, L. F.; NOGUEIRA, J. S.; DE OLIVEIRA, R. G.; LOBO, F. A.; VOURLITIS, G. L. Temporal patterns of energy balance for a Brazilian tropical savanna under contrasting seasonal conditions. **International Journal of Atmospheric Sciences**, v. 2013, p. 1-9, 2013. <https://doi.org/10.1155/2013/326010>
- ROERINK, G. J.; SU, Z.; MENENTI, M. A Simple Remote Sensing Algorithm to Estimates the Surface Energy Balance. **Physics and Chemistry of the Earth**, n. 25, p. 147-157, 2000. [https://doi.org/10.1016/S1464-1909\(99\)00128-8](https://doi.org/10.1016/S1464-1909(99)00128-8)
- SANTOS, C. A. C. D.; SATYAMURTY, P.; GOMES, O. M.; SILVA, L. E. M. G. D. Variability of extreme climate indices at Rio claro, São Paulo, Brazil. **Revista Brasileira de Meteorologia**, v. 27, n. 4, p. 395-400, 2012. <https://doi.org/10.1590/S0102-77862012000400003>
- SANTOS, J. R. N., DE ARAÚJO, M. L. S., JUNIOR, C. H. L. S., DOS SANTOS, J. S., ALMEIDA, J. L., LIMA, T. V., SOUZA, L.V. P.; AGUIAR, P. H. M.; SILVA, F. B. Tendências de extremos climáticos na região de transição Amazônia-Cerrado no Estado do Maranhão. **Revista Brasileira de Climatologia**, v. 26, p. 130-154, 2020. <http://dx.doi.org/10.5380/abclima.v26i0.62883>
- SENAY, G. B.; BUDDE, M.; VERDIN, J. P. ; MELESSE, A. M. A coupled remote sensing and simplified surface energy balance approach to estimate actual evapotranspiration from irrigated fields. **Sensors**, v. 7, p. 979-1000, 2007. <https://doi.org/10.3390/s7060979>
- SENAY, G. B.; BOHMS, S.; SINGH, R. K.; GOWDA, P. H.; VELPURI, N. M. Operational evapotranspiration mapping using remote sensing and weather datasets: a new parameterization for the SSEB approach. **Journal of the American Water Resources Association**, v. 49, p. 577- 591, 2013. <https://doi.org/10.1111/jawr.12057>
- SILVA, R. O. B.; MONTENEGRO, S. M. G. L.; SOUZA, W. M. Tendências de mudanças climáticas na precipitação pluviométrica nas bacias hidrográficas do estado de Pernambuco. **Engenharia Sanitária e Ambiental**, v. 22, n. 3, p. 579-589, 2017. <https://doi.org/10.1590/s1413-41522017142481>
- SILVA, W. L.; DEREZCZYNSKI, C.; CHANG, M.; FREITAS, M.; MACHADO, B. J.; TRISTÃO, L.; RUGGERI, J. Tendências observadas em indicadores de extremos climáticos de

- temperatura e precipitação no estado do Paraná. **Revista Brasileira de Meteorologia**, v. 30, n. 2, p. 181-194, 2015. <https://doi.org/10.1590/0102-778620130622>
- SOBRINO, J. A.; GOMEZ, M.; JIMENEZ-MUNOZ, J. C.; OLIOSO, A. Application of a simple algorithm to estimate daily evapotranspiration from NOAA-AVHRR images for the Iberian Peninsula. **Remote Sensing of Environment**, v. 110, p. 139-148, 2007. <https://doi.org/10.1016/j.rse.2007.02.017>
- SOUZA, A. P.; MOTA, L. L.; ZAMADEI, T.; MARTIN, C. C.; ALMEIDA, F. T.; PAULINO, J. Classificação climática e balanço hídrico climatológico no estado de Mato Grosso. **Nativa**, v. 1, n. 1, p. 34-43, 2013. <http://dx.doi.org/10.14583/2318-7670.v01n01a07>
- TANK, A. M. G. K.; ZWIERS, F. W.; ZHANG, X. **Guidelines on Analysis of extremes in a changing climate in support of informed decisions for adaptation**. World Climate Data and Monitoring Programme (WCDMP): 2009. 72 p.
- TASUMI, M.; ALLEN, R. G.; TREZZA, R. At-surface reflectance and albedo from satellite for operational calculation of land surface energy balance. **Journal of Hydrologic Engineering**, v. 13, p. 51-63, 2008. [https://doi.org/10.1061/\(ASCE\)1084-0699\(2008\)13:2\(51\)](https://doi.org/10.1061/(ASCE)1084-0699(2008)13:2(51))
- USGS - United States Geological Survey. **EROS Science Processing Architecture (ESPA)**. 2018. Disponível em: <<https://espa.cr.usgs.gov>>. Acesso em: 06 de julho de 2018.
- WANG, X. L.; WEN, Q. H.; WU, Y. Penalized maximal t test for detecting undocumented mean change in climate data series. **Journal of Applied Meteorology and Climatology**, v. 46, n. 6, 2007. <https://doi.org/10.1175/JAM2504.1>
- WANG, X. L. Accounting for Autocorrelation in Detecting Mean Shifts in Climate Data Series Using the Penalized Maximal t or F test. **Journal of Applied Meteorology and Climatology**, v. 47, p. 2423-2444, 2008. <https://doi.org/10.1175/2008JAMC1741.1>
- ZHANG, X.; YANG, F. **RclimDex (1.0) User Guide**. Climate Research Branch Environment Canada. Ontario: Downsview; 2004. 22 p.